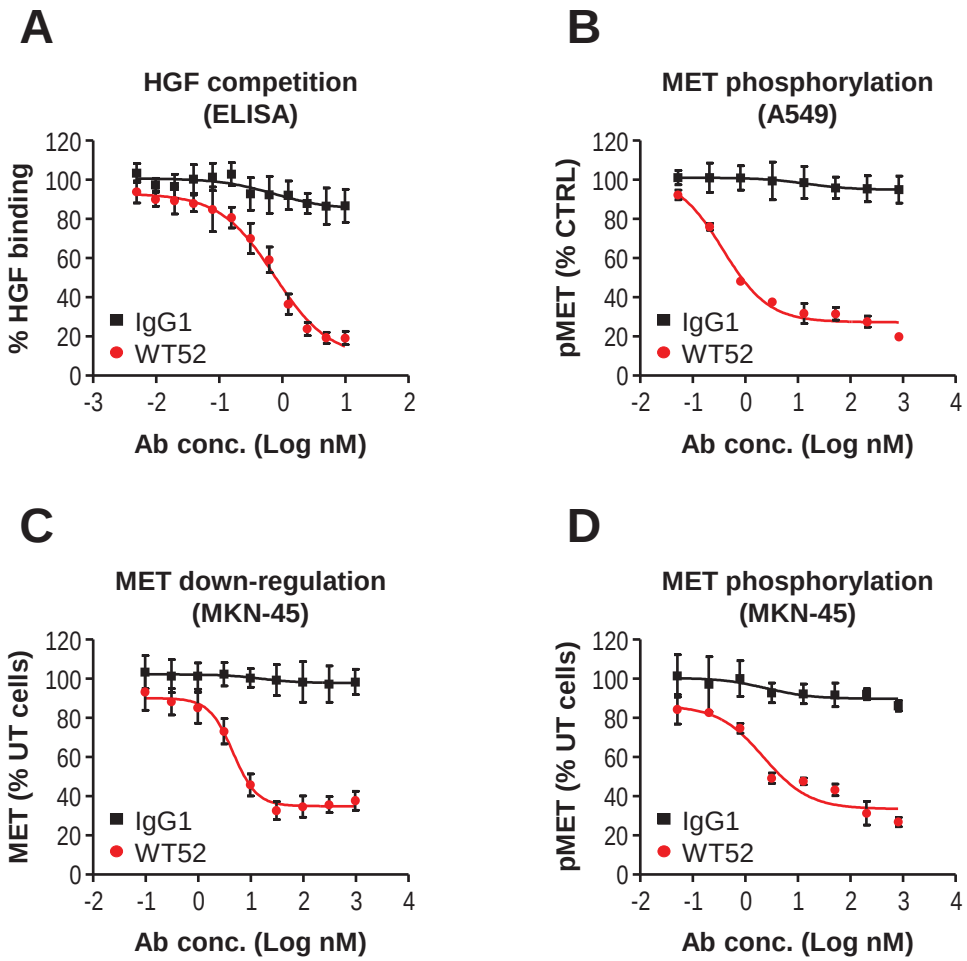


**Suppl. Fig. S1. WT52 inhibits both HGF-dependent and -independent MET auto-phosphorylation.** (A) HGF competition. Binding of HGF to a MET-Fc chimera was determined by ELISA in the presence of increasing concentration of WT52 or an irrelevant IgG1. Data are expressed as % binding relative to HGF alone. (B) Inhibition of HGF-dependent MET auto-phosphorylation. A549 human lung carcinoma cells, which express medium levels of MET and display ligand-dependent MET activation, were stimulated with HGF in the presence of increasing mAb concentrations. Phospho-MET (pMET) levels were determined by ELISA. Data are expressed as % pMET levels relative to cells stimulated with HGF alone. (C) MET down-regulation. MKN-45 human gastric carcinoma cells were incubated with increasing mAb concentrations, and MET levels were determined by flow cytometry. Data are expressed as % relative to untreated (UT) cells. (D) HGF-independent MET auto-phosphorylation. MKN-45 cells, which display c-*MET* gene amplification and constitutive MET activation, were incubated with increasing mAb concentrations, and MET auto-phosphorylation was determined as in A. Data are expressed as % pMET levels relative to UT cells.

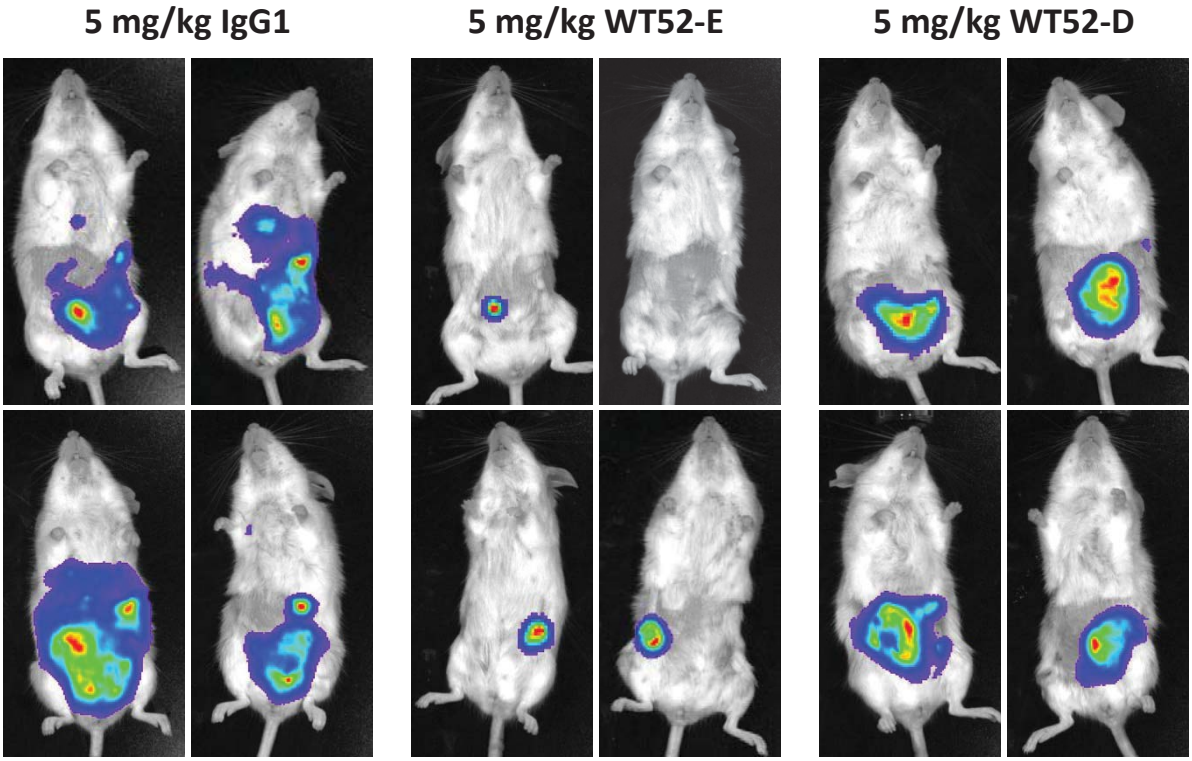


**Suppl. Fig. S2. MET-targeted ADCC prevents tumor recurrence and suppresses metastatic dissemination in an adjuvant orthotopic model of mammary carcinoma.** The therapeutic potential of MET-targeted ADCC was assessed in an adjuvant model of metastatic mammary carcinoma in which treatment started after tumor resection. MDA-MB-231-luc cells were injected orthotopically into the mammary fat pad of SCID mice, and primary tumors were removed by surgery approximately 5 weeks after cell injection. Two days after surgery, mice were randomized based on circulating tumor cell number and assigned to 3 treatment arms (IgG1, WT52-E, WT52-D). After 4 weeks of treatment, tumor regrowth and metastatic dissemination was assessed by whole body bioluminescence. The figure shows 4 representative images for each group. After imaging, mice were sacrificed and and isolated organs extracted for metastasis analysis (see Fig. 3).

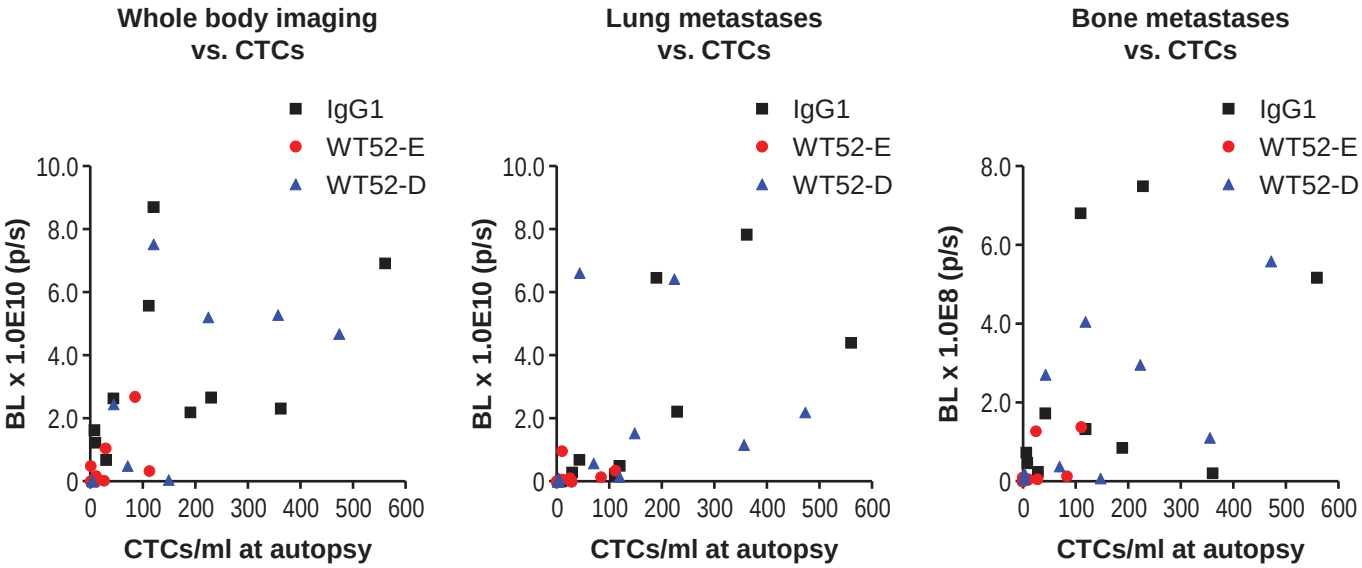


**Suppl. Fig. S3. Circulating tumor cell number shows direct correlation with the extent of metastatic dissemination.** Data from the experiment shown in Fig. 3 were analyzed for the corelation between the number of circulating tumor cells (CTCs) and metastatic dissemination. Metastases were determined by whole body imaging and by bioluminescence (BL) analysis of lungs and femurs.

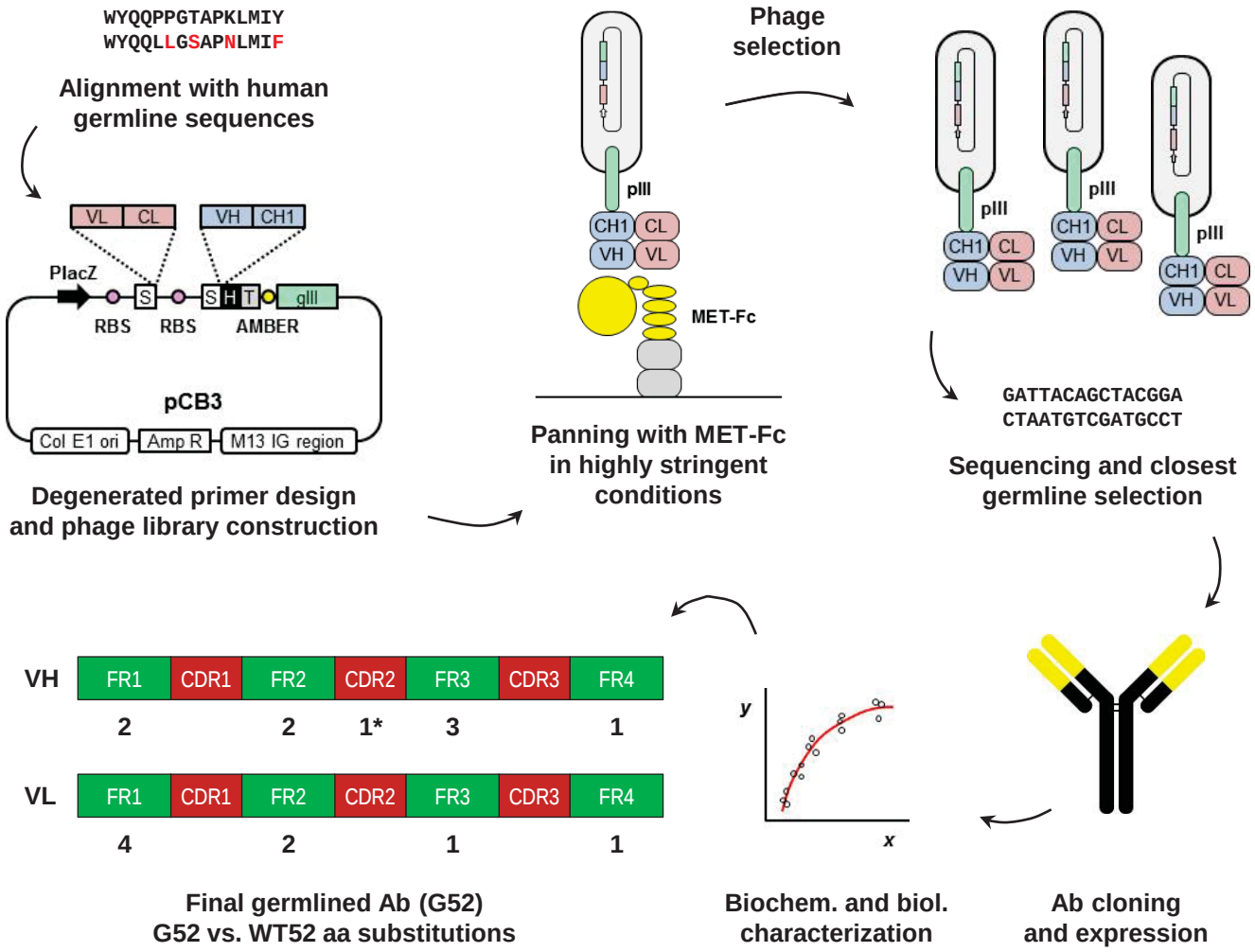


**Suppl. Fig. S4. Germlining of the WT52 antibody.** The variable regions of llama immunoglobulins display a surprisingly high degree of homology with their human orthologues. Therefore, germlining of llama antibodies is a much simpler procedure compared to humanization of murine antibodies: it does not involve CDR grafting, and requires only minor molecular modifications in the framework regions. Alignment of WT52 VH-VL sequences with human germline sequences revealed that this llama antibody displays 88% average framework human identity. Using degenerate primers for the creation of a synthetic germlined library and phage display-based affinity enrichment, we selected a molecule that displayed 95% human identity. The germlined antibody, G52, contained 9 amino acid substitutions in the VH region (one of which* was introduced to remove a de-amidation site) and 8 amino acid substitutions in the VL region. The numbers in the antibody scheme above indicate the amino acid (aa) substitutions in each variable region domain. FR1-4, framework regions 1-4; CDR1-3, complementarity determining regions 1-3.

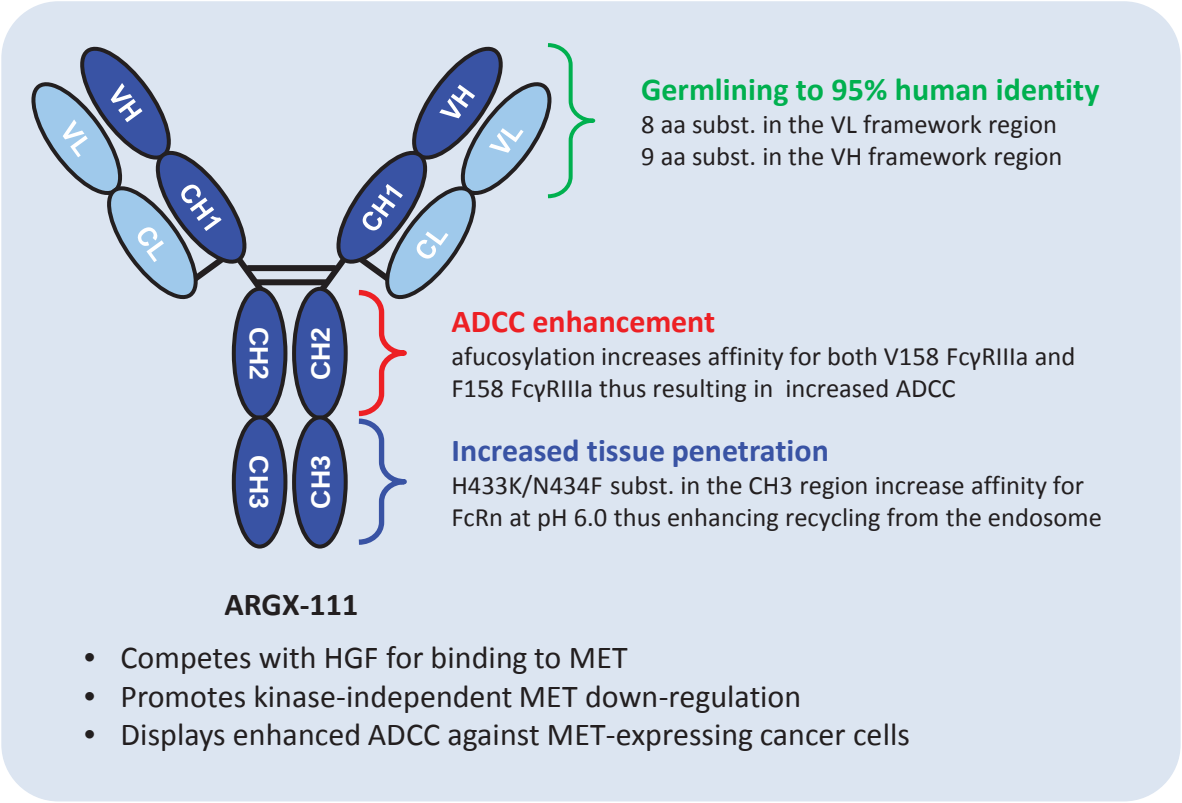


**Suppl. Fig. S5. ARGX-111, an antagonistic anti-MET antibody endowed with enhanced ADCC activity.** ARGX-111 was generated by genetic engineering of WT52, a chimeric llama-human antagonistic anti-MET antibody. ARGX-111 combines 3 distinct mechanisms of action: (i) it potently competes with HGF for MET binding, thus inhibiting ligand-dependent MET activity; (ii) it induces receptor down-regulation, thus curbing HGF-independent MET activity; (iii) it engages NK cells to kill MET-expressing cancer cells, thus displaying MET-specific cytotoxic activity.

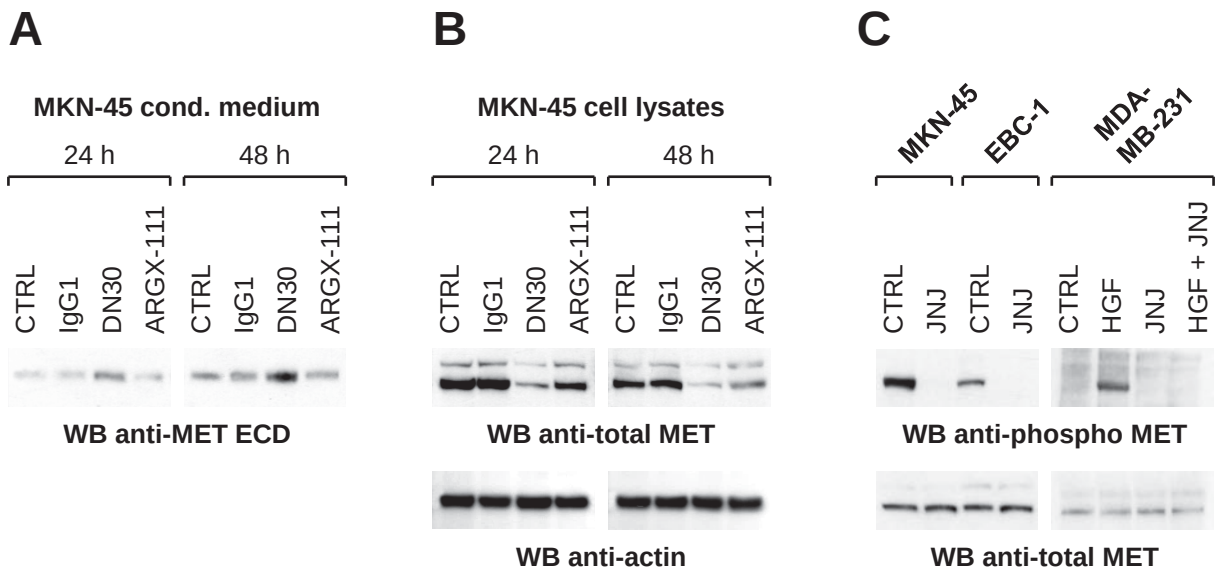


**Suppl. Fig. S6. ARGX-111 reduces total MET protein levels without promoting receptor shedding.** (A) MKN-45 cells were incubated with no factor, an irrelevant IgG1 antibody, the pro-shedding DN30 anti-MET antibody or ARGX-111 for 24 or 48 hours. Conditioned medium was analyzed by Western blotting (WB) using an antibody directed against the extracellular domain (ECD) of MET. (B) MKN-45 cells were incubated as in A and cell lysates were analyzed by Western blotting using anti-total MET antibodies or anti-actin antibodies. The upper MET band corresponds to the uncleaved MET precursor that is not exposed on the cell surface and does not typically undergo auto-phosphorylation. (C) MKN-45 and EBC-1 cells were incubated with no factor (CTRL) or the MET kinase inhibitor JNJ-38877605 (JNJ) for 24 hours, and cell lysates were analyzed by Western blotting using anti-phospho-MET antibodies and anti-total MET antibodies. MDA-MB-231 cells were cultured in the absence or presence of JNJ-38877605 for 24 hours and then stimulated with recombinant HGF for 10 minutes. Phospho-MET levels and total MET levels were determined by Western blotting as in B.

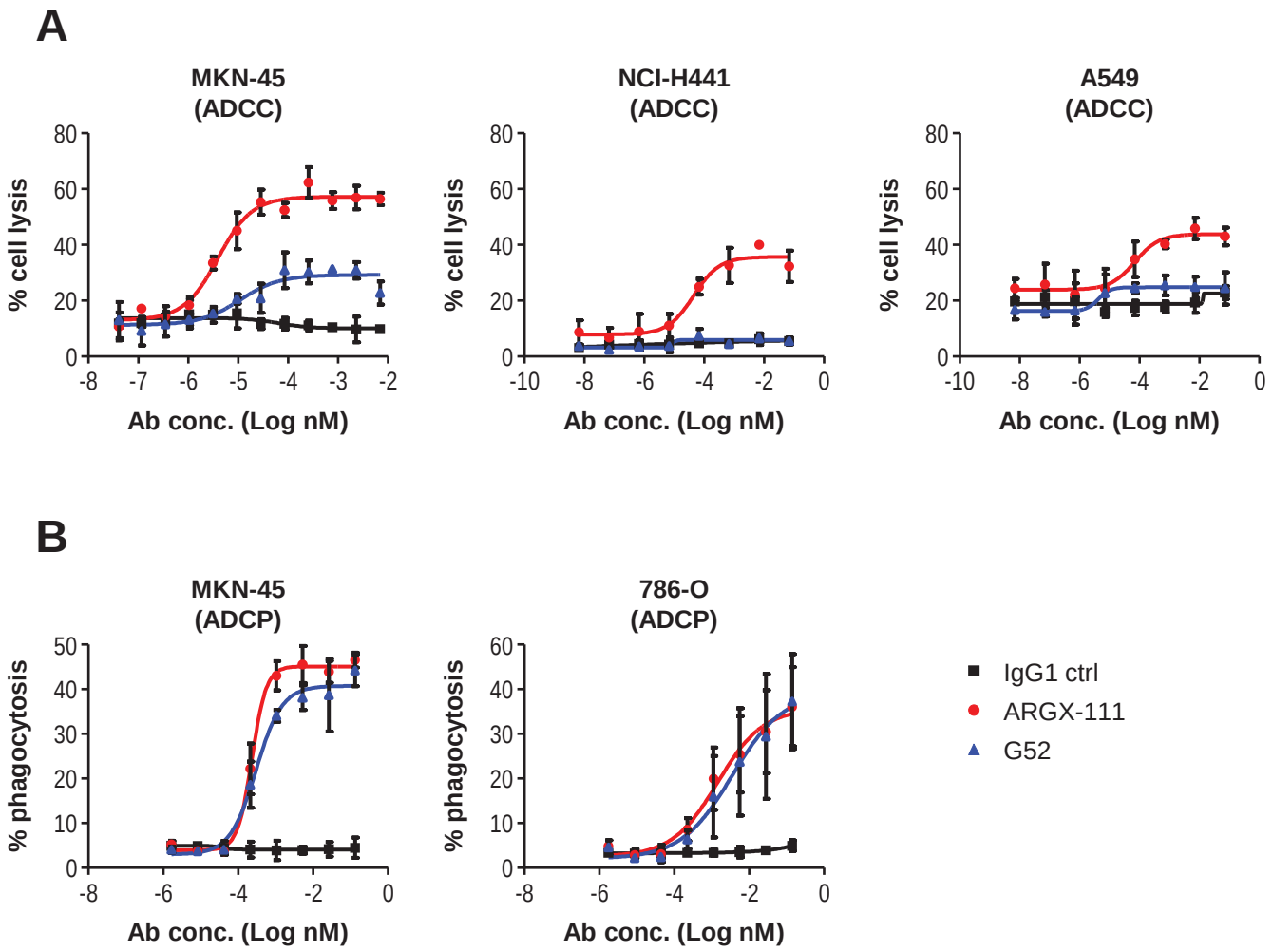


**Suppl. Fig. S7. ARGX-111 displays enhanced ADCC compared to fucosylated G52.** (A) The ability of ARGX-111 to kill cancer cells by ADCC was analyzed using the MKN-45, NCI-H441 and A549 human tumor cell lines. Cells were incubated with increasing concentrations of ARGX-111 in the presence of NK cells, and tumor cell lysis was determined by a standard $^{51}$Cr-release assay. An irrelevant IgG1 and the fucosylated G52 antibody were used as controls. Values represent the mean ± SD of 3 independent measurements. Each assay was repeated using effector cells derived from 3 different healthy donors. This figure shows the data from donor B. The complete set of data is shown in Suppl. Tab. S6. (B) The ability of ARGX-111 to induce antibody-dependent cell-mediated phagocytosis (ADCP) was analyzed using the MKN-45 and 786-O human tumor cell lines. Cells were incubated with increasing concentrations of ARGX-111, IgG1 or fucosylated G52 in the presence of human monocyte-derived machrophage cells, and phagocytosis was determined by flow cytometry. Values represent the mean ± SD of 3 independent measurements.